Double-exchange-driven spin pairing at the (001) surface of manganites

Alessio Filippetti* and Warren E. Pickett
Department of Physics, University of California at Davis, Davis, California 95616
(Received 27 July 2000)

Study of the (001) surface of the $La_{1-x}Ca_xMnO_3$ system in various magnetic orderings points to a general occurrence: z^2 dangling bond charge—which is ''invisible'' in the formal valence picture—is promoted to the bulk gap and/or Fermi level region. This unexpected occurrence, obtained from first-principles calculations, drives a double-exchange-like process that serves to align the surface Mn spin with its subsurface neighbor, regardless of the bulk magnetic order. For heavy doping, the locally ''ferromagnetic'' coupling is very strong and the moment enhanced by as much as 30% over the bulk value.

I. INTRODUCTION

Although most efforts on the colossal magnetoresistance (CMR) materials typified by the $La_{1-x}Ca_xMnO_3$ (LCMO) system are still concentrated on bulk properties, growing interest is being shown in the surface behavior.[1–3] Knowledge of surface properties is essential not only to develop a perovskite manganite-based technology but also to determine fundamental phenomena and mechanisms of magnetoelectronic behavior. The CMR effect occurs at relatively high temperature (around the magnetic ordering temperature), and a magnetic field of several Tesla is required to suppress the thermal magnetic disorder and produce the change in resistivity. Since high magnetic fields are generally unavailable in applications, alternative ways to trigger large low-field magnetoresistance (MR) were considered, such as with trilayer junctions[4] and polycrystalline samples.[5] The junctions are epitaxially grown along the [001] direction, and are made of a central insulating thin film of $SrTiO_3$ (the barrier), sandwiched by two metallic layers of $La_{0.67}Sr_{0.33}MnO_3$ (LSMO). Applying a low magnetic field, the tunneling conductivity can be switched by inducing a parallel (switch on) or antiparallel (switch off) spin orientation in the two electrodes. Taking advantage of their half metallicity gives a very large tunneling MR (TMR).

Large low-field intergrain MR (IMR) (Ref. 6) over a large temperature range has been observed in polycrystalline samples of LSMO,[6,7] CrO_2,[8] and the double perovskite systems $Sr_2Fe(Mo,Re)O_6$,[9,10] all of which are expected to be half metallic magnets. Magnetotunneling across grain boundaries, in which the relative orientation of the magnetization of neighboring grains is manipulated by an applied field, is believed to be the mechanism. In the IMR process, which may be the most promising for MR applications, there is mounting evidence that the state of the surface of the grains is important in the intergrain tunneling process.[7–9] For TMR it has long been clear that tunneling characteristics are strongly influenced, perhaps even dominated, by the electronic and magnetic structure at the interface, and for IMR surface states have been suggested to play the central role.

In the few experimental works present in the literature intrinsic difficulties have been reported in the process of obtaining clean, bulk-truncated surfaces, due to surface segregation that occurs during growth at high temperature,[3] and strain effects induced by film-substrate mismatch.[2] Structural and electronic properties of the low-index surfaces (including the possibility of reconstructions) are still unknown, in spite of their importance in establishing the half metallic nature of the CMR materials using photoelectron emission.[1] However, advancements in epitaxial growth and surface uniformity are being reported,[11] so a first fundamental step towards describing real surfaces consists in understanding how the intrinsic properties of the ideal unreconstructed surfaces differ from the respective bulk properties, i.e., how the bulk truncation in itself modifies the physics of the compounds. Particularly, in this paper we investigate the spin ordering of the magnetic Mn-terminated (001) surface of $La_{1-x}Ca_xMnO_3$.

First-principles calculations are particularly appealing for the study of surface properties. Indeed, the general reliability of local spin-density functional theory (LSDA), in conjunction with supercell methodologies, makes it possible to accurately and straightforwardly calculate quantities that are hardly accessible by experiments, such as surface formation energies, surface stresses and magnetic moments at surfaces. Also, peculiar to our methodology is the ability to predict the stable magnetic ordering by energy comparison of different possible magnetic phases. Here we take advantage of this predictive power to describe the mechanism of surface magnetic order stabilization, basically consisting of a change of spin ordering at surface with respect to the bulk ordering. Our LSDA calculations employ a plane-wave basis and Vanderbilt pseudopotentials.[12] A 30 Ryd cutoff energy and the exchange-correlation potential of Perdew and Zunger[13] was used.

Calculations for the Mn-terminated (001) surface of $x=1$ (i.e., $CaMnO_3$) has been presented in a previous paper.[14] There it was found that a robust magnetic surface stabilization was achieved by a spin-flip process on the Mn ions at the surface. Here we show that the same driving force that formed the basis of our prediction of the spin arrangement at the (001) surface of $CaMnO_3$ is still (or even more) dominant for other doping levels. Thus, although bulk $La_{1-x}Ca_xMnO_3$ shows an extremely rich variety of magnetic phases for different x,[15] a general behavior of spin ordering can be expected for the Mn-terminated (001) surface.

In Sec. II we report results of surface energies for different spin orderings, and in Sec. III an analysis of density of states and orbital occupations is presented.

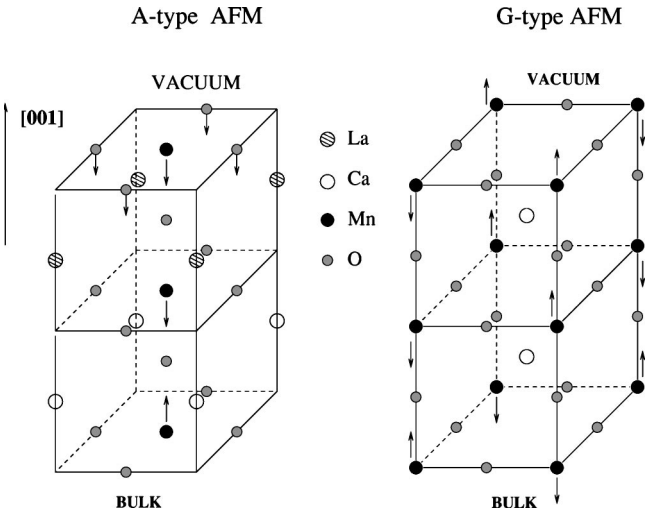

FIG. 1. Structure (half unit cell) of the (001) surfaces of tetragonal $La_{1/2}Ca_{1/2}MnO_3$ (left) and cubic $CaMnO_3$ (right). Arrows indicate spin orientations for the most stable magnetic ordering. With respect to the bulk ordering (A-type AFM for $La_{1/2}Ca_{1/2}MnO_3$, G-type AFM for $CaMnO_3$) the spin orientation on the surface Mn is reversed. Parallel alignment of the surface and subsurface layers is expected to be true generally. The surface oxygen ions are also polarized in $La_{1/2}Ca_{1/2}MnO_3$, but not in $CaMnO_3$.

II. MAGNETIC ORDERING AT THE (001) SURFACES OF $La_{1-x}Ca_xMnO_3$

In Fig. 1 the structure of the (001) Mn-terminated $La_{1-x}Ca_xMnO_3$ surfaces is shown for two levels of doping, i.e., for $La_{1/2}Ca_{1/2}MnO_3$ (left panel) and for $CaMnO_3$ (right panel). The bulk properties of these two compounds are quite different. The former has A-type antiferromagnetic (AFM) ordering, tetragonal symmetry, and in our calculation is a (poor) metal, whereas the latter is a cubic, G-type AFM, insulator. Thus, results for these two cases cover a sufficient variety of situations and allow us to draw conclusions about spin ordering of $La_{1-x}Ca_xMnO_3$ (001) surfaces applicable at any x.

The easiest case of the (001) surface of undoped $CaMnO_3$ has been fully understood in Ref. 14. We briefly describe the main findings. $CaMnO_3$ has G-type AFM bulk ordering due to standard AFM superexchange between filled t_{2g} shells. These t_{2g} shells contain the nominal three electrons assigned to Mn^{4+} in the formal valence picture, with the e_g formally empty. Actually, it has been pointed out elsewhere[16] that the real amount of d charge in transition-metal oxides is not at all identical to the formal d^n charge. Some e_g charge is present even in bulk $CaMnO_3$, resulting from $dp\sigma$ mixing that leads to strong hybridization of Mn e_g and O $2p$ bands.[17] However, the nominal ionic picture usually gives a reliable description of spin, charge, and orbital ordering.

Based on the growing understanding of the double-exchange (DEX) process in bulk manganites,[15] it can be expected that the surface spin alignment will be strongly dependent on the Mn e_g occupation. At the (001) surface the e_g degeneracy is broken: the x^2-y^2 orbital remains very strongly $dp\sigma$ hybridized with neighboring (in surface layer) O ions, but the z^2 orbital is left ''dangling.'' For $CaMnO_3$, G-type spin order does not survive at the (001) Mn-terminated surface. Instead, a flip of all the spins in the surface layer occurs, driven by the appearance of Mn z^2 charge localized in a narrow surface state whose energy lays within the bulk energy gap.[14] The filling of Mn z^2 orbital drives a DEX process that strongly favors the parallel alignment of spins on surface and subsurface nearest-neighbor Mn. In Fig. 1 the spin ordering of the stable phase of $CaMnO_3$ (001) surface is drawn by arrows on Mn. Mn ions on the second and third layers (the most bulklike) are G-type ordered, whereas spins on surface Mn ions are turned to be aligned with the subsurface Mn spins. Also, notice that flipping the spin of only one (out of two) surface Mn would produce a very unfavorable ferromagnetic (FM) ordering. Indeed, the surface formation does not substantially change the in-plane coupling that is as strongly AFM for the surface as for the bulk. Detailed results for $CaMnO_3$ can be found in Ref. 14. Here we want to assess that this spin-aligning mechanism survives, and in fact is enhanced, as doping occurs.

The results shown hereafter will be for the $La_{1/2}Ca_{1/2}MnO_3$ (001) Mn-terminated surface. In bulk $La_{1/2}Ca_{1/2}MnO_3$, the chemical picture is quite different from $CaMnO_3$. Indeed, Mn has (on average) d^4 occupation, and a partially occupied and broad e_g band mainfold lays between the occupied $t_{2g}^{\uparrow}$ and empty $t_{2g}^{\uparrow}$ bands. The e_g occupation generally causes the occurrence of dramatic changes (orbital and charge ordering arise, driving the system toward C-type magnetic orderings.[18]) In our calculations we cannot take into account the bulk with the true spin, charge, and orbital ordering of the $x=1/2$ compound (that is beyond the current first-principles computational capabilities). Nevertheless, the behavior at the surface that we identify is so robust that we expect it to be rather independent of the bulk magnetic order.

Thus, we chose to represent $La_{1/2}Ca_{1/2}MnO_3$ in a (1×1) tetragonal symmetry, made by alternating layers of La and Ca orthogonal to the $\hat{z}$ axis. The bulk AFM phase is then described by a four-layer (i.e., two formula units) cell, with antialigned spins on the two Mn (i.e., the so called A-type AFM). In this configuration, we obtain (by energy minimization) a bulk lattice constant $a_0=7.21$ a.u, which is a very reasonably middle value between the experimental 7.35 a.u. for $La_{2/3}Ca_{1/3}MnO_3$, and 7.05 a.u. for $CaMnO_3$. Also, the AFM phase is favored by 15 meV/Mn over the FM, which has a nearly half-metallic density of states. For the surface we used a slab of nine atomic layers (a half slab is shown in Fig. 1, left panel), retaining a mirror symmetry with respect to the central Mn layer. The artificial ordering of La and Ca layers (which must be somehow arbitrarily fixed in a finite supercell approach) does not affect our conclusions, since cations Ca and La do not contribute to the bonding other than by donating their valence electrons to the O and Mn bands. In this tetragonal symmetry there are two kinds of Mn-terminated (001) surfaces, one with La in the subsurface layer (indicated as Mn-La, and drawn in Fig. 1), and another with Ca instead (Mn-Ca).

In Table I the calculated surface energies are reported. We see that Mn-La and Mn-Ca surfaces give almost equivalent results. This indicates that energetics and magnetic order at the surface are barely sensitive to the chosen stoichiometry and symmetry.

For each of the two surfaces, four spin arrangements on Mn are possible, labeled in Table I by triplets of arrows representing the spin orientation on central (C), subsurface

TABLE I. Energies (in meV) for different spin configurations on Mn atoms. Each of them is labeled by three arrows indicating the spin direction of central-subsurface-surface Mn. Mn-La is the Mn-terminated (001) surface with La on the second layer, Mn-Ca is that one with Ca on the second layer. All energies refer to that of the most stable arrangement, i.e., $\uparrow\downarrow\downarrow$.

C-SS-S	$\uparrow\uparrow\uparrow$	$\uparrow\uparrow\downarrow$	$\uparrow\downarrow\uparrow$	$\uparrow\downarrow\downarrow$	J_{S-SS}	J_{SS-C}	J_{S-C}
Mn-La	23	144	91	0	53	−18	8
Mn-Ca	17	142	88	0	53	−18	9

(SS), and surface (S) Mn (in the order). For example, $\uparrow\uparrow\uparrow$ is the configuration with all the spins aligned, $\uparrow\downarrow\downarrow$ the configuration with the spin on subsurface layer antialigned with that one of the central layer, and aligned with the spin at surface, and so on. We find the $\uparrow\downarrow\downarrow$ spin alignment strongly favored overall, i.e., the stable configuration is that one with the spin orientation at the surface reversed with respect to the bulk-truncated A-type AFM ordering.

The energies can be mapped onto an interlayer Ising model with three independent effective exchange constants (Table I): J_{S-SS}, J_{SS-C} and J_{S-C}, the latter being a second-neighbor coupling. $J_{SS-C}=-18$ meV (AFM) is close to the exchange parameter obtained directly from the bulk calculation ($J_{bulk}=-15$ meV). The interaction between Mn on first and third layers, $J_{C-S}=8$ meV, is FM in sign. It is related to the d_{z^2} surface state that will be discussed in the following section. The most striking result of Table I is the positive, unusually large value of $J_{S-SS}=53$ meV, more than three times larger than, and opposite in sign to, the bulk AFM coupling. For comparison, for $CaMnO_3$ the interlayer exchange constant at the surface was 29 meV.[14] (The bulk coupling for $CaMnO_3$ is $J_{bulk}=-26$ meV.) This large FM coupling between surface and subsurface Mn for both $x=1$ and $x=1/2$ compounds is the consequence of a very general characteristic of the (001) surface formation, and can be understood in the light of a careful analysis of the density of states.

III. DENSITY OF STATES AND ORBITAL OCCUPATIONS

Since Mn-La and Mn-Ca give equivalent results, in this section we present calculations for just one of them (Mn-La). In Fig. 2 the orbital-resolved density of states (DOS) of the Mn ions for the (001) surface in the most stable spin configuration (i.e., $\uparrow\downarrow\downarrow$) is shown. The three panels refer to the three inequivalent Mn ions placed into one half of the surface slab (see Fig. 1). With our method (i.e., plane-wave basis and pseudopotentials), this resolved DOS can be obtained by projections of Bloch states onto the basis of pseudo-atomic orbitals. At variance with the real-space integration over atomic-centered spheres usually performed within the linear-augmented plane-wave framework, our approach does not discard eventual interstitial contributions.

For the sake of clarity, the d_{z^2} DOS in Fig. 2 is drawn by a shaded area. Two surface Mn d_{z^2} DOS peaks straddle the Fermi energy ($E_F=0$), with a tail of occupied states that extends down to ~ -1.5 eV. These states are also visible on subsurface Mn and, marginally, on central Mn as well. Thus the surface formation produces a deep surface state with d_{z^2} orbital character at E_F extending to the fifth layer below the surface. This surface state has been similarly found on the (001) surface of $CaMnO_3$ (Ref. 14) and (we believe) it would arise at any doping level.

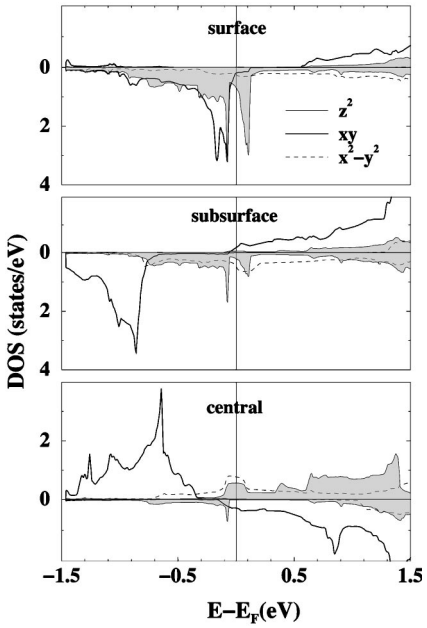

FIG. 2. Orbital-resolved Mn *d* DOS for the (001) Mn-La surface in the spin configuration $\uparrow\downarrow\downarrow$ (see text). The different panels refer to the three unequivalent Mn into the slab, placed (from top to bottom panel) on surface, subsurface, and central layer. To be better distinguished, the DOS of the crucial d_{z^2} surface state is drawn by a shaded area.

In the majority channel of the central (bulklike) Mn ion, d_{z^2} and $d_{x^2-y^2}$ orbitals contribute to the DOS at E_F, whereas in the minority channel the only contribution comes from t_{2g} states. It is also apparent that the surface d_{xy} bands are shifted upward in energy with respect to the bulk. Indeed, the minority channel at surface is depleted by $d^{\uparrow}_{xy}$ bands (i.e., Mn at surface is fully polarized), and the $d^{\downarrow}_{xy}$ bands of surface Mn contribute to the DOS at E_F. The magnetic moment on the surface Mn ($3.23\mu_B$) is 10% larger than on subsurface Mn ($2.97\mu_B$) and 30% larger than in the central Mn ($2.50\mu_B$), but the total charge on Mn (~ 5.3 electrons using our methodology) is nearly the same at the surface and in the bulk. The increase of magnetization is mostly due to the d_{z^2} polarization, with some contribution from the depletion of $d^{\downarrow}_{xy}$ states around E_F. Also, a small intra-atomic charge readjustment occurs from $d_{x^2-y^2}$ and d_{xy} to the polarized d_{z^2} orbital on surface Mn.

The polarization at the surface can be visualized from the isosurfaces of the magnetization density displayed in Fig. 3. Two isosurfaces with equal magnitude but different sign (dark and light surfaces represent up and down magnetization, respectively) are shown. To obtain this magnetization we sum up only states whose energy lies in the region within 0.3 eV below E_F. In such a way (see Fig. 2), the dominant contribution of the ''core'' t_{2g} states to the magnetization is not included in the isosurfaces surrounding Mn, and the smaller e_g contributions are made evident.

Consistently to the DOS analysis, the surface Mn shows a combination of d_{z^2} and d_{xy} orbitals, whereas on subsurface

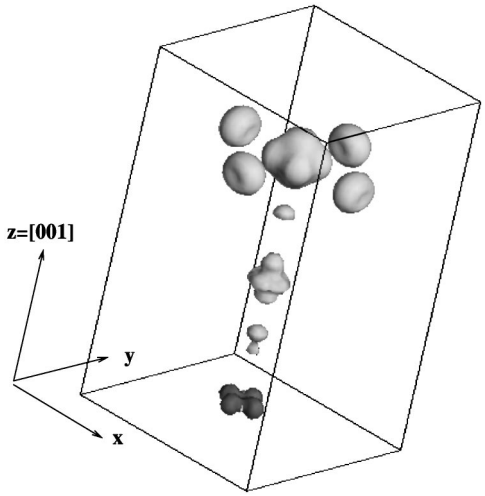

FIG. 3. Isosurfaces of the magnetization density for the (001) Mn-La surface in the spin configuration $\uparrow\downarrow\downarrow$. Dark and light isosurfaces are of same magnitude but opposite sign, i.e., they represent up and down spin densities, respectively. Only states of energy below, and within, 0.3 eV of E_F contribute to the isosurfaces (see the corresponding DOS in Fig. 2).

Mn the d_{z^2} magnetization is mixed with some $d_{x^2-y^2}$ character. The double-exchange effect between d_{z^2} orbitals on surface and subsurface Mn comes into play and leads to the strong FM coupling ($J_{S-SS}=53$ meV) responsible for the spin alignment. On central Mn the magnetization is $d_{x^2-y^2}$-like. (Unfortunately, present computational limitations do not allow us to study an 11-layer slab, for which the central layer should be more bulklike.) Also evident in Fig. 3 is that a remarkably large fraction of this surface-induced magnetization lies in the O p_π orbitals of the surface layer (the corresponding magnetic moment is $\sim 0.15\mu_B$). Polarization of O in FM bulk manganite perovskites has been emphasized elsewhere.[19]

The change of the Mn d_{z^2} orbital from broad, strongly $dp\sigma$ hybridized in the bulk to an atomiclike, narrow in energy, surface state is a very specific feature of this (001) surface formation, and this surface dehybridization generally should be described well by LSDA. We suggest that this effect is strong enough to turn the AFM spin coupling between the top two layers into FM for any doping level. At least two arguments support this hypothesis. First, the spin pairing occurs for the (001) surface of $CaMnO_3$,[14] which should be the most unfavorable case, since in the bulk (nominally) only the majority t_{2g} orbitals are occupied, thus their AFM character is particularly dominant. Nevertheless, the partially occupied d_{z^2} surface state reverses the magnetic coupling. Second, the very large change of exchange interaction parameter (from -15 meV in bulk to $+53$ meV at the surface) would overcome AFM bulk coupling even stronger than the one considered here.

A crucial case is the $x=0$ member $LaMnO_3$, which is A-type AFM in the bulk. The spin-pairing argument applied to the (001) FM surface predicts a spin flip on the surface Mn. The AFM spin coupling along the $\hat{z}$ axis is robust and explained by a well established picture: the in-plane FM coupling is stabilized by the ordering of Mn e_g orbitals, so that occupied d_{x^2} (d_{y^2}) orbitals alternates with empty d_{x^2} (d_{y^2})

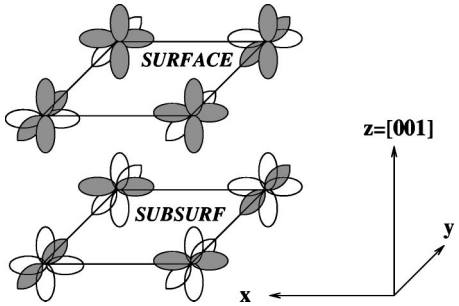

FIG. 4. Orbital ordering at $LaMnO_3$ (001) surface: filling of d_{z^2} orbital (indicated by shading) at the surface produces FM spin coupling perpendicular to the surface. Planar orbital ordering in the subsurface and other buried layers leads to FM layers alternating in spin direction, except at the surface.

orbitals on neighboring Mn. Thus, all the e_g-type charge fills in-plane orbitals, and the AFM interactions between neighboring t_{2g}'s dominates in the orthogonal direction.

A realistic first-principles calculation of the $LaMnO_3$ surface is beyond our possibility, since it would require a $\sqrt{2}\times\sqrt{2}$ lateral enlargement of the cell as well as additional thickness to treat the tilting of the MnO_6 octahedra[20] and the Jahn-Teller distortion at the surface. However, the formation of the d_{z^2} surface state within the bulk $LaMnO_3$ gap seems to be beyond doubt, based on the behavior of the d_{z^2} dangling bond for $x=1$ and $x=1/2$. The question is whether this would be able to overcome the t_{2g} AFM contribution.

To this end, useful information is provided by Ref. 21. Here, the t_{2g} contribution to J_{bulk} in $LaMnO_3$ has been calculated as a function of c/a, i.e., of the distortion between in-plane and interplanar lattice constants at fixed volume, and it was found to increase linearly in magnitude with the distortion. In other words, the AFM coupling between (001) planes increases linearly by shortening the interplanar distance, likely due to the electrostatic repulsion that further depletes the d_{z^2} orbitals. However, the variation of this t_{2g} contribution over a wide range of c/a values is in the range of ~ 20–30 meV, i.e., not large enough to overcome the value of J_{S-SS}. This behavior supports our expectation of the occurrence of a spin-flip process at the (001) $LaMnO_3$ surface as well.

Finally, in Fig. 4 we show a schematic picture of the e_g orbitals on surface and subsurface layers, indicating the expected filling and orbital ordering after the formation of the surface state. The orbitals are ordered both in-plane and orthogonally to the surface, as a result of the surface formation that fills the surface Mn d_{z^2} orbital, no longer degenerate with the d_{z^2} orbital of the underlying subsurface Mn.

IV. SUMMARY

In this paper we have shown that terminating the (001) surface of $La_{1-x}Ca_xMnO_3$ with the Mn ion exposed, results in a partial filling of the d_{z^2} orbital that drives a double-exchange-like ordering of the magnetic moments of surface and subsurface Mn. We have shown this effect explicitly for $x=1/2$ and (previously) for undoped $CaMnO_3$. A comparison between these two cases indicates that the surface-induced FM coupling is stronger in doped systems. This re-

sult has important implications (1) for surface studies, where this effect tends to ensure that surfaces of the CMR materials ($x \approx 1/3$) will remain ferromagnetically aligned and half metallic as well, as supported by photoemission studies, and (2) for the intergrain magnetoresistance effect, where the magnetic structure of the grain surfaces can strongly affect the device characteristics. This behavior, which is strongly related to band filling but much less dependent on ion size effects, should also hold for the $La_{1-x}Sr_xMnO_3$ and $La_{1-x}Ba_xMnO_3$ systems.

ACKNOWLEDGMENTS

This research was supported by National Science Foundation Grant No. DMR-9802076. Calculations were done at the Maui High Performance Computing Center.

*Present address: Materials Department, University of California, Santa Barbara, Ca 93106-5050.

[1] J.-H. Park, E. Vescovo, H.-J. Kim, C. Kwon, R. Ramesh, and T. Venkatesan, Phys. Rev. Lett. **81**, 1953 (1998).
[2] H. B. Peng, B. R. Zhao, Z. Xie, Y. Lin, B. Y. Zhu, Z. Hao, H. J. Tao, B. Xu, C. Y. Wang, H. Chen, and F. Wu, Phys. Rev. Lett. **82**, 362 (1999).
[3] J. Choi, J. Zhang, S.-H. Liou, P. A. Dowben, and E. W. Plummer, Phys. Rev. B **59**, 13 453 (1999).
[4] Y. Lu, X. W. Li, G. Q. Gong, G. Xiao, A. Gupta, P. Lecoeur, J. Z. Sun, Y. Y. Wang, and V. P. Dravid, Phys. Rev. B **54**, 8357 (1996); J. Z. Sun, L. Krusin-Elbaum, P. R. Duncombe, A. Gupta, and R. B. Laibowitz, Appl. Phys. Lett. **70**, 1769 (1997).
[5] A. Gupta, G. Q. Gong, G. Xiao, P. R. Duncombe, P. Lecoeur, P. Trouilloud, Y. Y. Wang, V. P. Dravid, and J. Z. Sun, Phys. Rev. B **54**, 15 629 (1996).
[6] H. Y. Hwang, S.-W. Cheong, N. P. Ong, and B. Batlogg, Phys. Rev. Lett. **77**, 2041 (1996).
[7] S. Lee, H. Y. Hwang, B. I. Shraiman, W. D. Ratcliff, and S-W. Cheong, Phys. Rev. Lett. **82**, 4508 (1999).
[8] H. Y. Hwang and S.-W. Cheong, Science **278**, 1607 (1997).
[9] K.-I. Kobayashi, T. Kimura, Y. Tomioka, H. Sawada, K. Terakura, and Y. Tokura, Phys. Rev. B **59**, 11 159 (1999).
[10] T. H. Kim, M. Uehara, S-W. Cheong, and S. Lee, Appl. Phys. Lett. **74**, 1737 (1999).
[11] M. Kawasaki, M. Izumi, Y. Konishi, T. Manako, and Y. Tokura, Mater. Sci. Eng., B **63**, 49 (1999).
[12] D. Vanderbilt, Phys. Rev. B **32**, 8412 (1985); K. Laasonen, A. Pasquarello, R. Car, C. Lee, and D. Vanderbilt, *ibid.* **47**, 10 142 (1993).
[13] J. P. Perdew and A. Zunger, Phys. Rev. B **23**, 5048 (1981).
[14] A. Filippetti and W. E. Pickett, Phys. Rev. Lett. **83**, 4184 (1999).
[15] *Physics of Manganites*, edited by T. A. Kaplan and S. D. Mahanti (Kluwer/Plenum, New York, 1999).
[16] R. E. Cohen, Nature (London) **358**, 136 (1992).
[17] The 18 O p bands of bulk $CaMnO_3$ actually contain on the order of 1.5–2 electrons of Mn e_g character.
[18] I. V. Solovyev and K. Terakura, Phys. Rev. Lett. **83**, 2825 (1999).
[19] W. E. Pickett and D. J. Singh, Phys. Rev. B **53**, 1146 (1996).
[20] J. B. A. A. Elemans, B. van Laar, K. R. van der Veen, and B. O. Loopstra, J. Solid State Chem. **3**, 238 (1971).
[21] I. Solovyev, N. Hamada, and K. Terakura, Phys. Rev. Lett. **76**, 4825 (1996).